

Real-time Bandwidth Estimation from Offline Expert Demonstrations

Aashish Gottipati¹, Sami Khairy², Gabriel Mittag², Vishak Gopal², and Ross Cutler²
¹University of Texas at Austin, ²Microsoft

Abstract

In this work, we tackle the problem of bandwidth estimation (BWE) for real-time communication systems; however, in contrast to previous works, we leverage the vast efforts of prior heuristic-based BWE methods and synergize these approaches with deep learning-based techniques. Our work addresses challenges in generalizing to unseen network dynamics and extracting rich representations from prior experience, two key challenges in integrating data-driven bandwidth estimators into real-time systems. To that end, we propose *Merlin*, the first purely offline, data-driven solution to BWE that harnesses prior heuristic-based methods to extract an expert BWE policy. Through a series of experiments, we demonstrate that *Merlin* surpasses state-of-the-art heuristic-based and deep learning-based bandwidth estimators in terms of objective quality of experience metrics, while generalizing beyond the offline world to in-the-wild network deployments where *Merlin* achieves a 42.85% and 12.8% reduction in packet loss and delay, respectively, when compared against WebRTC in inter-continental videoconferencing calls. We hope that *Merlin*'s offline-oriented design fosters new strategies for real-time network control.

1 Introduction

Estimating the optimal rate of information flow is essential to ensuring congestion-free network communication. The bottleneck link— the link with the least available bandwidth—dictates the rate of information flow across the network. Estimating the bottleneck link refers to the problem of bandwidth estimation (BWE)— a challenging and active area of networking research. BWE is fundamental to real-time communication (RTC) systems and lies at the heart of network systems. Without accurate bandwidth estimates, seamless network communication becomes nearly impossible.

The challenge of BWE emerges from the complex and dynamic nature of network environments [52]. First, network flows change over time as devices come and go and users change applications, resulting in a non-stationary environ-

ment with the bottleneck link varying over time. Second, the bottleneck link often lies beyond the first hop and cannot be probed instantaneously. Third, network environments are partially observable. That is, many outside factors such as cross-traffic impact the bottleneck link and cannot be directly controlled. To chip away at these challenges, early bandwidth estimators in RTC relied mainly on Real-time Transport Protocol (RTP) [46], which probes the network and aggregates receive-side network statistics. By periodically probing the network via RTP, the effects of non-stationarity and partial observability can be mitigated when estimating the capacity of the bottleneck link. The simplicity of RTP enables portability; however, it limits the quality of estimates produced [28], leading to the widespread adoption of more sophisticated heuristic-based methods [7].

Based on aggregated network statistics, rule-based estimators such as WebRTC [4] leverage statistical models to estimate the available bandwidth. While these methods have been widely adopted, increasing network heterogeneity and complexity necessitates more sophisticated methods. For example, RTC applications such as videoconferencing require high bandwidth and low latency while passive internet-of-things (IoT) monitoring systems require low bandwidth. Both of these flows, while disparate in their requirements, compete for resources in the network core. Scaling to millions or even billions of flows, resources quickly become scarce while flow interactions perturb the network. To better serve users and meet growing resource demands, we require fine-grain network control, i.e., instantaneous adaption to network changes. However, prior rule-based methods tend to follow longer-term network trends to promote smooth estimates [4]. Additionally, heuristic-based models were hand-crafted based on extensive domain knowledge, making them difficult to adapt to the ever-changing network landscape. Lastly, even with domain knowledge, network complexity is quickly outstripping human intuition, e.g., configuring a simple TCP session has dozens of free variables [9]. To enable future network applications, we require methods that react to instantaneous network changes, cope with the growing complexity of networks, and

are easy to update.

Within recent years, deep learning-based models have demonstrated impressive ability for real-time adaption under complex domains, while enabling ease of updates through enhanced input data and fine-tuned objective functions [39]. Although these properties are desirable, real networks tend to be extremely diverse, making data-driven adoption difficult. In contrast to other deep learning methods, reinforcement learning (RL) seeks to learn a policy. The learned policy incorporates environment dynamics, enabling the learned agent to grasp not only which control actions are positive but which are negative as well. RL utilizes exploration to search over control policies, enabling the agent to try unconventional strategies and discover robust network control policies [24]. Even so, RL agents are conventionally trained from a blank slate in on-line environments, neglecting the vast amount of knowledge encoded in previous heuristic-based methods, and requiring a large number of training samples to converge to an acceptable policy. In the case of videoconferencing, the large sample complexity translates to hundreds of thousands of videoconferencing calls and extremely long convergence times [13]. Second, and most crucially, in videoconferencing we seek to learn a policy to maximize user quality of experience (QoE); however, defining a reward for subjective user experience with objective network metrics is difficult and remains an open research problem. Furthermore, without a well-defined reward function, agents may exploit the reward definition and maximize the expected return without learning the desired task— a phenomenon known as reward hacking [19]. To that end, we desire a method for real-time BWE that exhibits the benefits of deep RL but leverages the vast efforts of prior domain experts; thus, we turn towards offline imitation learning (IL) methods.

IL differs from RL in that it seeks to learn a policy from a known expert, i.e., given a set of offline demonstrations (expert states and actions), extract a policy that best fits the expert. IL builds upon the vast efforts of previous domain knowledge encoded within heuristic-based experts and enables many of the benefits of RL. However, there is no free lunch. Imitating an expert for real-world BWE suffers from two distinct challenges. First, extracting a policy from a finite set of expert demonstrations does not necessarily result in the true generalizable, expert policy. Without extracting the true policy, the agent is likely to introduce compounding errors under unseen dynamics, severely degrading user QoE [60]. Secondly, hand-crafted expert feature representations may not necessarily translate directly to data-driven methods [14]. Consequently, we propose *Merlin*, the first purely offline, data-driven solution for BWE that harnesses the encoded domain knowledge of prior methods to extract an expert BWE policy. *Merlin* is trained to imitate an expert Unscented Kalman Filter (UKF) model strictly from offline, simulated demonstrations via behavioral cloning (BC), a method that reduces policy learning to supervised learning. **We emphasize that no network inter-**

actions are required to train *Merlin* and data is collected once before training. Furthermore, as expert demonstrations are sampled strictly from simulation, **we require no specialized hardware or testbed environments to generate data for our agent**, democratizing access to learning-based network control.

We rigorously evaluate *Merlin* in simulated, testbed, and wild environments. The highlights of our evaluations are as follows. We find that our IL model outperforms the state-of-the-art heuristic-based methods as well as the state-of-the-art RL-based methods in terms of objective QoE metrics within our emulated testbed. Furthermore, we demonstrate that our imitator is robust to domain shifts and is capable of mimicking our expert UKF model with high confidence in emulated environments. We further support our claims with in-the-wild deployments, where *Merlin* achieves a 42.85% and 12.8% reduction in packet loss and delay, respectively, while preserving a higher receive rate in comparison to WebRTC in inter-continental videoconferencing calls. Lastly, we observe that the reported receive rate and media type features are critical to extracting a control policy. Increasing the number of demonstrations appears to aid in mitigating domain shift but was not directly reflected in IL loss metrics. Leveraging temporal correlations via recurrent models tends to perform better than non-recurrent methods. Lastly, when expert demos are abundant, BC tends to outperform more sophisticated IL methods.

In summary, our contributions are as follows:

1. We demonstrate a new method for BWE that utilizes IL to extract expert policies from purely offline data, leveraging the extensive domain expertise encoded in prior hand-crafted network heuristics.
2. We rigorously evaluate *Merlin* in simulated, emulated, and real-world conditions to study the generalization of cloned policies. Our analysis provides insights into achieving robustness to distribution shift, a key challenge in adapting data-driven models.
3. We conduct multiple ablation studies to uncover IL best practices for network control. Our guidelines on features, demonstrations, and architectures provide a recipe for future research at the intersection of machine learning and networking.
4. We discuss the broader potential of learned policies to transition toward data-driven control for non-stationary networked systems. IL shows promise for flexibly modeling complex network dynamics offline.

Overall, we position this work as advancing the integration of machine learning techniques into networking systems.

2 Related Work

Congestion control (CC) solutions broadly seek to promote packet flow, reducing network congestion while encourag-

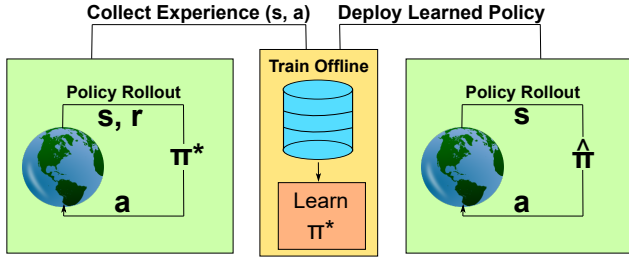


Figure 1: Learning from Offline Demonstrations.

ing maximum bandwidth utilization. These approaches often employ BWE to measure the available link capacity and set the send rate accordingly. Classical techniques for BWE have traditionally relied on various forms of packet probing techniques [21]; however, these methods are fundamentally limited by probing overhead which may itself contribute to congestion. More modern approaches employed sophisticated statistical techniques to estimate bandwidth [27, 56]. Most notably, implementations of WebRTC [4] utilize a Kalman Filter for BWE and have become the de facto standard for RTC. While widespread, heuristic-based methods tend to be conservative, matching long-term trends rather than tracking instantaneous network perturbations [7, 13].

Other methods have sought to take a broader approach to CC for RTC systems. For example, enforcing a close coupling between video codecs and the transport layer has been shown to reduce network congestion by jointly adapting the encoding rate of video frames and the transport layer send rate [16, 69]. More recent endeavors have shifted to machine learning and deep learning techniques to estimate bandwidth by exploiting the structured signal present in network data [25, 47, 55, 59]. While traditional deep learning techniques tend to perform well for static tasks such as classification, they struggle to adapt to more dynamic control tasks such as CC, which requires learned dynamics to inform congestion decisions [1].

Incorporating network dynamics enables learning richer BWE and CC policies. Accordingly, recent works have sought to apply reinforcement learning to CC [5, 18, 22, 33, 40, 43, 48, 57, 58, 67]. Mao et al. [38] learn a policy to dynamically tune the transmit rate of video packets and deploy their learned model on Facebook’s web-based video streaming platform; however, their area of focus is confined to video-on-demand and not RTC systems. On the other hand, the first RL-based bandwidth predictor for RTC systems, R3Net [13], relied exclusively on deep RL to produce bandwidth estimates, neglecting prior domain expertise. Other novel RL-based approaches to CC exploit cross-layer features to inform policy decisions [8, 30, 34, 35, 37, 66]; however, enforcing a close-coupling between layers restricts architecture design and reduces modularity.

In contrast, recent works have sought to leverage expert algorithms for model training. Eagle [11] adopts an expert-oriented approach, seeking to match BBR [6] via online RL. DuGu [23] utilizes an online IL approach to mimic a custom

CC oracle for short-term video uploads. Zhou et al. propose Concerto [68], a BC-based method that leverages oracle estimates to select the best video bitrate from a discrete set of encodings; however, we emphasize we focus on learning to estimate the available network resources from offline domain-expertise collected from prior heuristic-based methods.

Later works such as Gemini [61], HRCC [54], HybridRTS [65], BoB [3], SAFR [62], OnRL [64], and Libra [10] build non-standalone estimators directly on top of heuristic-based methods or utilize prior methods as fall-back mechanisms to mitigate tail-end predictions of learned agents. Along similar lines, Zhang et al. explore fusing cloned experts with online RL-based models for video bitrate prediction [63]. In contrast to these works, we propose *Merlin* a standalone, data-driven approach to BWE that does not rely on auxiliary estimators such as Google’s Congestion Control (GCC) algorithm for BWE.

Lastly, the most similar work to ours is Sage [60]. Sage builds upon the vast efforts of prior methods for learning a purely, data-driven TCP-based CC algorithm via offline RL. In contrast to Sage, we emphasize that we tackle the problem of BWE for RTC systems rather than CC for TCP-based applications; hence, the dynamics of our problem are dissimilar, e.g., TCP-based systems maintain reliability while RTC systems exchange reliability for reduced latency. Furthermore, no specialized testbed equipment nor even emulated interfaces are required for model training. *Merlin* is trained completely from offline simulated experience, enabling others to readily build on our method.

In summary, *Merlin* differs in fundamental ways from prior works. First, we do not utilize RL or hybrid methods and rely on IL to learn a standalone BWE policy. Second, as depicted in Figure 1, we train purely offline without ever interacting with a network during training, generalizing from offline simulated experience to both emulated and wild environments. Lastly, *Merlin* is designed specifically for RTC systems, prioritizing latency over reliability.

3 Bandwidth Estimates vs. User Experience

To illustrate the importance of BWE, we conducted a preliminary study on the impact of bandwidth estimates on user QoE during RTC videoconferencing. We benchmark three bandwidth estimators: our expert UKF model, an overshooter, and an undershooter. We conduct approximately 100 live videoconferencing calls on real networks and report the video mean opinion score (MOS), a gold standard metric for video QoE that ranges from one to five with one corresponding to low QoE and five mapping to high QoE [41]. We report a subset of our findings from network environments with stable 1 Mbps links in Figure 2. In Figure 2a, the bandwidth estimator overshoots the 1 Mbps limit, which causes the video MOS to severely degrade, oscillating between 0.0 and 2.0 (a MOS of 0 indicates an error, i.e., no video frames are received). The

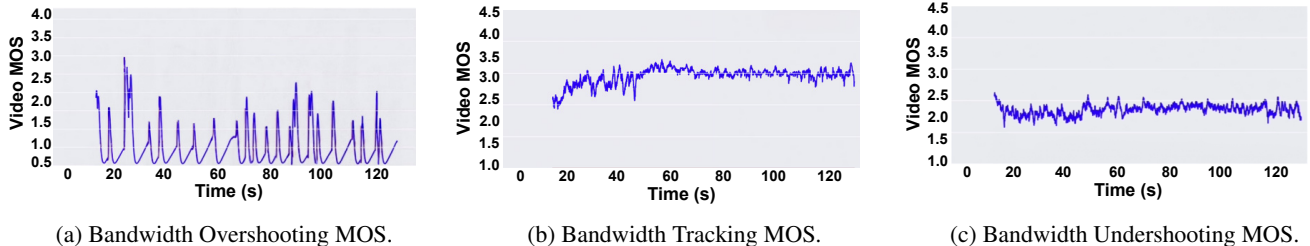


Figure 2: Quality of Bandwidth Estimates vs. User Experience.

poor bandwidth estimates severely degrade objective QoE and cause the sender to flood the network with packets, resulting in increased queuing delays and packet loss.

In contrast to overshooting, in Figure 2c, the bandwidth estimator severely underestimates the 1 Mbps link. Although not as harsh as overshooting, the video MOS degrades due to a lack of high-quality video frames, resulting in a stable MOS of 2.0. Specifically, the video codec leverages the bandwidth estimates to choose an encoding rate for each frame. By underestimating the available bandwidth, the video frames are encoded at a reduced bitrate to meet bandwidth requirements, delivering lower-quality video streams to the receiver. However, since the network is not congested, packets are still able to flow freely and arrive at the receiver without being lost, leading to better user experience and a higher MOS than in the overshoot case.

Lastly, we observe the best video MOS when the bandwidth estimator tracks the bandwidth closely as demonstrated by our UKF expert in Figure 2b. By providing accurate resource estimates, packets are able to flow freely without being dropped; additionally, video frames can be encoded at higher bitrates due to the increase in estimated network resources. The increased video encoding rate translates to higher-quality video streams being delivered to the receiver which results in a stable MOS of 3.0. In comparison to undershooting and overshooting, tracking the available bandwidth closely leads to a significant boost in objective QoE. We report the results on simple stable cases to illustrate the impact of bandwidth estimates; however, BWE becomes more challenging in live environments due to the partial observability and non-stationary nature of real networks [52]. Thus, in this work, we seek to tackle complex environments. We conduct several videoconferencing experiments on live inter-continental links in section 5, and demonstrate that we can preserve user QoE through high-quality BWE via purely offline IL.

4 Merlin

Design Goals. Conventional bandwidth estimators provide smooth estimates over long horizons, making instantaneous network adaptation difficult. In contrast, new RL-based estimators react promptly to network perturbations and are “easy” to update but often exhibit high sample complexity and require a well-defined reward function to guide network control policy.

Thus, we desire a method for real-time BWE that exhibits the benefits of deep RL but leverages the vast efforts of prior domain experts to bypass reward definitions; thus, we turn towards offline IL. Specifically, we seek to leverage BC to extract an expert BWE policy from offline expert demonstrations for real-time BWE.

Overview. For our work, we seek to mimic our expert UKF model, a rule-based model constructed from extensive domain expertise. UKF, like WebRTC, adopts a delay-based approach; that is, based on observed network delays, UKF smoothly adapts its bandwidth estimates. More concretely, UKF utilizes an internal dynamics model to represent the current network state and a set of static functions to adapt its bandwidth estimate. In contrast to WebRTC, UKF was designed specifically for videoconferencing. The estimates produced by UKF do not follow an additive increase multiplicative decrease (AIMD) scheme, which leads to smoother bandwidth estimates in comparison to WebRTC’s “sawtooth” behavior. UKF has previously been deployed on Microsoft Teams; hence, it is a battle-tested expert for real-time bandwidth estimation. Additionally, as extensive domain expertise is required to adjust UKF, it is the perfect candidate for our work. Thus, given a set of collected UKF demonstrations Ξ , UKF states S , and UKF actions $\pi^*(s)$, we seek to learn the expert policy π^* in the following manner:

$$\pi^* = \arg \min_{\pi} \sum_{\xi \in \Xi} \sum_{s \in S} L(\pi(s), \pi^*(s)) \quad (1)$$

where π corresponds to the policy of our imitator.

By reframing policy learning in the context of supervised learning, BC enables agents to learn a control policy while benefiting from the stability and convergence properties of supervised learning. Despite these benefits, BC suffers from the problem of compounding error [53]. Supervised learning relies on the i.i.d. assumption which may not hold during long-horizon tasks. Trajectories contain a sequence of states and actions that often depend temporally, breaking the i.i.d. assumption [45]. As a result, when a BC model arrives at an unseen state, the newly executed action may be misaligned with the true objective, diverging slightly from the expert trajectory. The dependence between states causes the error to compound as the BC agent moves along its trajectory, diverging more and more from the expert. Compounding error

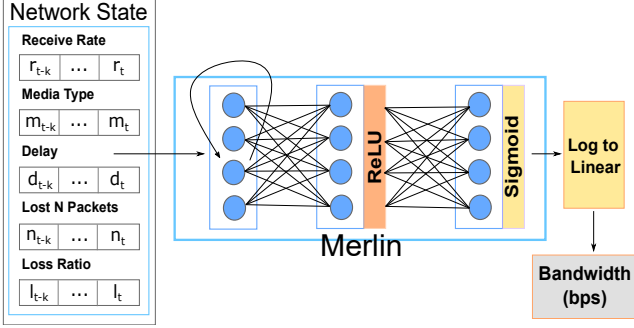


Figure 3: Merlin’s Network Architecture.

has been shown to limit the robustness of BC models as the learned agents are incapable of bridging to new unseen environments [60]. To tackle real-world applications, IL methods must also overcome the distribution shift between offline demonstrations and target environments.

Addressing Compounding Error. To combat compounding error and improve generalization, we utilize a large number of expert demonstrations. We utilize OpenNetLab’s gym environment to collect expert trajectories. Specifically, we collect 100k expert demonstrations from simulation, randomly varying the call parameters to improve data diversity. By sampling the expert from a diverse set of circumstances, Merlin is able to better observe the expert from a variety of states, which enhances state space coverage and mitigates compounding error. Furthermore, to mitigate the effects of compounding error that may arise due to the sheer size of the output range, we restrict bandwidth estimates to 10 Kbps and 8 Mbps, a range that supports audio-only calls to high-definition videoconferencing calls with screen sharing. We additionally limit our action space \hat{b}_{log} to a real number between 0 and 1 and employ a log transform to project Merlin’s output action into bps,

$$\hat{b}_{log} = \frac{\log(\hat{b}) - \log(b_{min})}{\log(b_{max}) - \log(b_{min})} \quad (2)$$

where \hat{b} represents the estimated bandwidth, b_{min} corresponds to the minimum bandwidth, b_{max} is the maximum bandwidth, and all bandwidth values are in Mbps. Limiting the action space to a number between 0 and 1 reduces the complexity of our action space and helps our model learn a more robust policy. The impact of these design decisions is reflected in the results detailed in section 5.

Extracting BWE Signals in Partially Observable Environments. To deal with partial observability, state-of-the-art heuristic-based methods such as WebRTC combine queuing theory with raw network metrics to model one-way delay gradients for BWE [7]. In contrast, current RL methods start from a blank slate and learn to extract complex BWE signals from raw network metrics. Both methods, while performant, neglect the benefits of each other; that is, heuristic-based methods are fundamentally limited by the capacity of domain

experts and cold-start RL overlooks prior efforts. Accordingly, Merlin is designed to learn these domain-specific representations implicitly through expert supervision via IL. Similarly, Merlin relies on its data-driven architecture to extrapolate more complex signals; specifically, we incorporate a Long Short Term Memory (LSTM) unit to maintain the history of previous network behavior. The LSTM acts as a buffer for experience, and, over the duration of a videoconferencing call, Merlin builds up its internal state representation to learn temporally-dependent features that capture the non-stationary nature of the network environment. The robustness to partial observability is validated in section 5.

In addition to incorporating expert supervision and learned feature representations, we conducted an exhaustive feature ablation study detailed in section 5 to arrive at the best performing state representation (detailed in Appendix A). Most notably, we experimented with including the five previous bandwidth estimates which were sampled at 60 ms granularity. However, as we utilize offline expert trajectories for training, these estimates actually correspond to our expert’s previous predictions. It was observed that these features hindered Merlin’s ability to extract the expert policy. We hypothesize that the previous estimates led to Merlin placing more weight on these previous estimates; effectively, “cheating” by reusing UKF estimates for bandwidth prediction. Thus, when generalizing to new environments, Merlin would perform poorly in comparison to our expert UKF model. Pruning these previous estimates greatly enhanced Merlin’s robustness to domain shift.

Tackling Domain Shift. As previously mentioned, prior heuristic methods were constructed by domain experts; hence, updating these models is non-trivial. The current process for updating these methods relies on a time-consuming processing and entails collecting network statistics, manually hand-engineering representations, and redeploying these heuristics, repeating until an acceptable measure of success is achieved. As network heterogeneity increases, specializing these models for individuals and adapting model parameters to each new environment quickly becomes infeasible. On the other hand, RL agents can be readily fine-tuned with new observations; however, estimates tend to be noisier, reacting to instantaneous network perturbations. In contrast, Merlin utilizes IL for expert supervision to mitigate overly aggressive reactions to network perturbations, effectively regularizing bandwidth estimates. In combination with expert supervision, Merlin’s state construction utilizes both short term and long horizon features to promote smooth bandwidth estimates. As a first step, IL enables learning a policy for smooth expert bandwidth estimates, while the data-driven design facilitates a personalized experience by fine-tuning on new observations. Merlin’s resilience to domain shift is empirically validated by generalizing from offline simulated observations to real, inter-continental videoconferencing calls, an environment where state observations deviate significantly from offline experi-

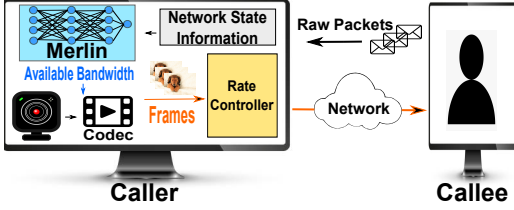


Figure 4: System overview of Merlin.

ence, in section 5. Merlin’s architecture and policy network are described next.

Architecture Details. We choose to utilize an LSTM for our policy network to exploit the temporal correlations present in network traffic and mitigate compounding error. We benchmark against non-recurrent architectures in section 5. Our findings demonstrate that the recurrent structure of the LSTM enhances network control performance by exploiting the temporal dependencies between network control actions. Merlin accepts a 64 length tensor of normalized state observations. As depicted in Figure 3, Merlin first encodes state observations with its LSTM and then leverages two fully-connected layers to decode state observations into output actions. The first fully-connected layer is followed by a ReLU activation function while the final output layer utilizes a sigmoid activation function, limiting the model output to a real number between 0 and 1. It is important to note that we utilize a small, lightweight architecture for client-side deployment and real-time execution (≈ 60 ms granularity).

Training Procedure. As illustrated in Figure 5, we train Merlin from offline UKF demonstrations. First, we deploy our expert UKF in a fork of OpenNetLab’s gym environment [12]. The gym leverages the WebRTC stack and NS3 [44] to simulate videoconferencing calls to promote data-driven BWE solutions. Network behavior is simulated according to the provided trace workloads and network parameters. Our calls are generated from a diverse set of production traces, encompassing low bandwidth, high bandwidth, fluctuating bandwidth, burst loss, and LTE workloads. During generation, we randomly vary call parameters such as the proportion of video packets to audio packets, queuing delays, and the video start times. At each step in the simulation, transport layer information such as the send time, arrival time, and payload size is reported. The gym environment provides tools for calculating relevant transport metrics such as the delay, loss ratio, and receiving rate from the exposed packet level information.

We record the observed packet level information and UKF bandwidth predictions from 100k unique calls. We apply the inverse of equation 2 to project UKF’s bandwidth estimate into action space for training. It is important to note that gym packets do not contain real video and audio payloads; hence, there is a gap between real and simulated videoconferencing calls. The sim-to-real gap limits the breadth of expert demonstrations; however, the programmatic nature and cus-

tomizability of call parameters enable us to collect expert demonstrations from a diverse set of circumstances that may not be realizable under real-world conditions. Although our expert is not observed in real-world environments, we emphasize that the diverse set of observations enables our model to bridge the gap from simulated networks to in-the-wild deployments.

Before training, an offline dataset of state observations was constructed by grouping packets received in 60 ms windows and aggregating feature-level information accordingly. Features were reconstructed based on the state representation detailed in Appendix A. The sequence of states and actions from one call was treated as a single training sample. To train Merlin, a batch size of 256 was utilized, i.e., 256 calls were ingested per training step. The mean squared error (MSE) between Merlin’s actions and UKF’s expert actions was minimized over the course of 1000 training epochs. Different loss functions such as mean-absolute-error (MAE) were empirically tested, indicating that the MSE loss objective produced the best imitation policy. To update model parameters and dynamically tune the learning rate, Adam optimization was employed with an initial learning rate of 0.001. After each training epoch, utilizing randomly generated videoconferencing workloads and OpenNetLab’s gym, the MSE validation performance between Merlin and UKF was reported (see Section 5 for more details on workload generation). **Most importantly, Merlin never interacted with a network nor was a single packet transmitted during train time. Furthermore, training data was collected once— prior to training.**

Implementation. We implement Merlin’s LSTM architecture in Pytorch. We export Merlin to ONNX format and utilize ONNX runtime for deployment. ONNX provides a basic model wrapper that enables compatibility across operating systems and applications. Merlin can be deployed directly into the Teams media stack via ONNX runtime for receiver-side estimation. By extracting an expert policy from offline experience, we succeed in building upon prior heuristic-based estimators for BWE. That is, we utilize the encoded domain knowledge to learn a generalizable, data-driven bandwidth estimator without ever transmitting a single network packet.

5 Evaluation

In this section, we seek to answer the following questions:

1. Is offline, simulated experience alone sufficient to produce expert bandwidth estimates?
2. How robust is the learned BWE policy to domain shift?
3. Which features are most important to mimicking an expert estimator?
4. How do different IL architectures and techniques impact bandwidth estimates?
5. How does the quantity and quality of demonstrations affect BWE performance?

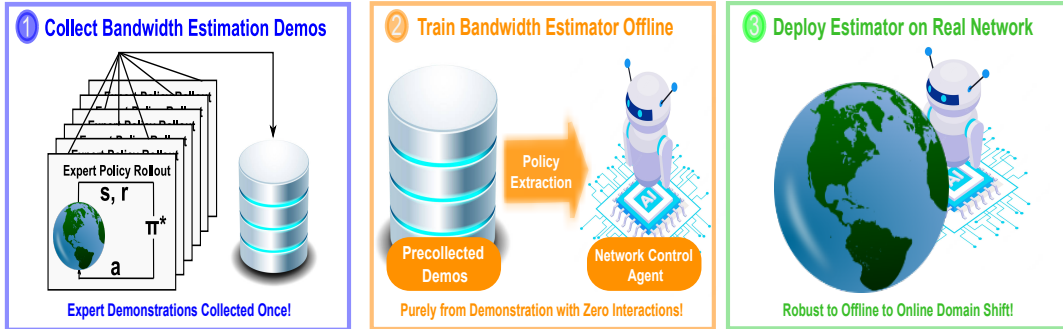


Figure 5: From Offline Demos to Agent Deployment, Training Merlin via Imitation Learning.

5.1 Methods

Environment Assumptions and Parameters. For our evaluations, we sample state observations at 60 ms granularity, enabling real-time BWE. Bandwidth estimates are clipped to be between 10 Kbps and 8 Mbps, which supports a broad range of RTC applications, ranging from audio-only calls to high-definition, 30 frames per second videoconferencing with interactive screen sharing. Estimates below 10 Kbps are below industry recommendations for audio-only calls, while estimates above 8 Mbps offer no added benefits. Lastly, we restrict our evaluations to peer-to-peer, audio and video calls (see Figure 6) and leave group calls for future work.

Benchmarks. We benchmark against two different state-of-the-art bandwidth estimators. (1) WebRTC [4], the de facto standard for RTC applications that utilizes GCC for BWE. GCC leverages a Kalman filter to tune bandwidth estimates based on the estimated end-to-end one-way delay variation [7], employing an AIMD scheme. WebRTC is the most widely utilized communication stack for RTC applications. (2) R3Net v1.4, a variant of the online RL model proposed by Fang et al. in [13]. R3Net v1.4 was previously benchmarked against HRCC [54] and Gemini [61], the winners of MMSys ’21 Bandwidth Estimation Challenge, and shown to outperform both models, achieving state-of-the-art performance for RL-based BWE. In addition to baseline comparisons, we evaluate Merlin’s imitation quality in relation to our expert UKF, a custom, hand-engineered statistical model previously deployed in production on Microsoft Teams.

Metrics. For our simulated evaluations, we track the MSE between Merlin and UKF in action space as our sole key performance indicator. A small action MSE indicates that the actions produced by our BC model closely match those produced by UKF, while a larger difference indicates a deviation between the imitator and the expert. While calls are simulated, the simulated packets do not carry any meaningful payload, so we do not compute gold-standard metrics such as the video MOS in this environment.

In contrast to our simulated environments, we track the following metrics in our testbed and wild environments. (1) Video MOS. The MOS values range from 1 to 5 with 1 indicating poor QoE and 5 indicating exceptional QoE. Video

MOS is the gold standard for QoE and is computed based on user feedback. In our work, we utilize a vision-based model to produce a video MOS estimate [41]. The estimates were shown to exhibit 99% correlation with user visual experience. (2) Audio MOS. Similar to the video MOS, the audio MOS also ranges from 1 to 5 with 1 indicating low audio QoE and 5 indicating high QoE. Audio MOS is the gold standard for audio-based QoE and is computed based on user feedback. In our work, we utilize a signal-based model to produce an audio MOS estimate. The estimates were internally shown to correlate significantly with user audio experience. (3) Receiving rate. The receiving rate is reported in Kbps and correlates with user experience. While a higher receiving rate is preferred, delay and packet loss must be taken into account as a high receiving rate can correlate with network congestion. (4) Packet loss rate. The percentage of lost packets observed. A lower loss rate indicates that packets are freely flowing through the network while a high loss rate indicates network congestion and degradation in user QoE. (5) Delay. The delay metric is reported in ms, with a lower delay indicating higher QoE and a higher delay indicating network congestion. We choose to track the delay mean as opposed to the delay MOS, as a notable shift in delay is required to move the delay MOS score significantly, e.g., 3 ms increase in delay corresponds to an observed 0.001 increase in delay MOS (a higher delay MOS is worse). Furthermore, it is important to note that while multiple network metrics correlate to user experience, the relationship is complex. Thus, to understand the overall impact on user experience, we must analyze these metrics collectively rather than individually.

Simulated Evaluation. We evaluate the performance of Merlin against UKF using traces generated from production parameters within a fork of OpenNetLab [12]. We randomly generate traces for evaluation from a diverse set of network workloads containing low bandwidth, high bandwidth, fluctuating bandwidth, burst loss, and LTE. Call parameters such as the proportion of video packets to audio packets, queue delay, and the video start time are randomly sampled at runtime. Our evaluation consists of 480 distinct simulated calls. We run 1000 validation runs, which corresponds to nearly 480,000 simulated calls. We report the best achieved performance.

It is important to note that in real videoconferencing calls, video packets are not received at the start of the call. This is because audio packets tend to flow first, which leads to a sharp change in bandwidth once video packets are received. Our randomly generated traces capture the variation in delay of video streams. This shift in bandwidth leads to more challenging traces for BWE.

Testbed Evaluation. We benchmark the performance of `Merlin` against WebRTC, UKF, and R3Net v1.4 using production traces over emulated networks within our testbed environment. We utilize 10 different production traces which cover low bandwidth, high bandwidth, fluctuating bandwidth, and burst loss settings. Our testbed consists of two lab machines connected over a network link. The network link is emulated to match production settings. Since we are transmitting over real networks, other factors such as cross-traffic and queuing delays influence the results of our evaluation. To mitigate noise, we conduct hundreds of evaluation calls and utilize a Welch t-test to determine whether our results are statistically significant. Our evaluation consists of over 100 emulated calls per model (≈ 400 calls in total at 10 per trace). We report the averaged metrics across each network profile. In relation to UKF, we seek to accept the null hypothesis, that is, there is no difference between the performance of the imitator and the expert within our emulated environment. In contrast, we seek to outperform existing methods such as WebRTC and R3Net v1.4.

In the Wild Evaluation. We measure the performance of `Merlin` against UKF and WebRTC over real networks in the wild. Our setup consists of 20 nodes distributed across North America, Asia, and Europe. For each evaluation call, we randomly sample 10 pairs of nodes. We then conduct calls with UKF, WebRTC, and `Merlin`. We conducted our experiments during the day and at night over the course of a week. Similar to our emulated evaluation, we conducted hundreds of evaluation runs and utilized a Welch t-test to determine whether our results were statistically significant. Our evaluation consists of over 700 in the wild calls per model (≈ 2100 calls in total). We report the averaged metrics across all runs. In relation to UKF, we seek to accept the null hypothesis, that is, there is no difference between the performance of the imitator and the expert within real deployments. In contrast, we seek to improve upon WebRTC.

Ablation Studies. We experiment with different learning parameters and evaluate our imitator against UKF using randomly generated workloads within our simulated environment. The setup is identical to our simulated evaluations. We report the best achieved performance across each parameter setting. We experiment with different architectures, IL methods, input features, demonstration numbers, and types of demonstrations. For an in-depth review of the IL methods tested, we direct readers to Appendix E.

Key Findings. Through our evaluations, we demonstrate the following findings:

1. Offline experience is sufficient to produce expert bandwidth estimates. `Merlin` outperforms the state-of-the-art bandwidth estimators in terms of video MOS, audio MOS, and the average receiving rate. We show that the change in video MOS and receiving rate are statistically significant. `Merlin` also shows no statistical movement in comparison to UKF on real networks.
2. Our learned BC policy is robust to domain shift. We train on offline experience from simulated UKF calls and generalize to both emulated and wild networks. We further show that these results are statistically significant by showing no movement in terms of video MOS and audio MOS.
3. The most important features for mimicking an estimator and producing expert bandwidth estimates are the receiving rate and the media type features. Counter-intuitively, we find that the average packet loss rate and loss ratio have little effect on the learned predictor. The best subset of features contains all five input feature categories.
4. Rather than using demonstrations drawn from our target environment, we find that the richness and diversity of demonstrations contributes more to the performance of the imitator; hence, using a diverse set simulated data is sufficient for policy extraction.

5.2 Simulated Audio and Video Calls

We first assess the ability of `Merlin` to imitate our expert UKF bandwidth estimator. `Merlin` achieves an MSE difference of 0.0012 in action space in comparison to UKF over 480 randomly generated traces (see LSTM-BC in Figure 10b). While opaque, these results indicate that `Merlin` can closely mimic our expert UKF estimator which is evident in our qualitative assessment in Figure 7. Most notably, in Figure 7a, we see that `Merlin` inherits the same quirks as our expert. UKF takes a more conservative approach to BWE to produce smoother estimates over the duration of the videoconferencing call; as a result, UKF avoids abrupt changes that are prominent in the fluctuating case. Furthermore, our expert produces estimates based on the observed packets, and since video packets tend to not flow immediately, our expert severely undershoots the true bandwidth at the beginning of the high bandwidth call in Figure 7b. Since audio packets only require 10 Kbps of bandwidth, both the expert and imitator severely undershoot the true bandwidth at the beginning of the call; however, as soon as bandwidth-hungry video packets begin to flow across the network, both the imitator and UKF exhibit the same behavior of smoothly ramping up to the bandwidth limit. Both quantitatively and qualitatively, we demonstrate that our imitator is capable of mimicking our expert from purely offline experience within simulation. Our simulation mainly serves as a validation check that our imitator works as expected. We discuss more rigorous evaluations in the coming evaluation sections.

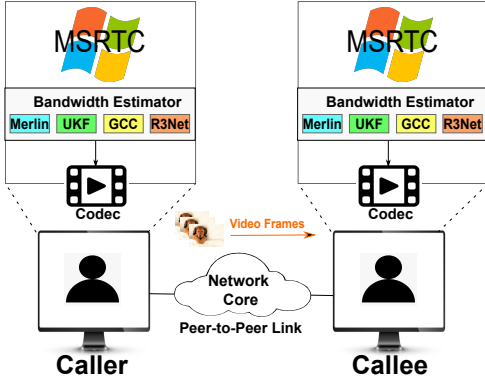


Figure 6: Deploying estimators on videoconferencing clients.

5.3 Testbed Videoconferencing

We compare the performance of our learned imitator against three benchmark models: WebRTC, UKF, and R3Net v1.4 over controlled networks with emulated links. We note that cross-traffic and other noise contributors are present within the testbed environment. We test each estimator across a diverse set of production network traces and aggregate statistics across ≈ 100 calls for each method. Our results are summarized in Table 1. In terms of video MOS scores, *Merlin* outperforms both WebRTC and R3Net v1.4, two state-of-the-art methods. *Merlin* achieves a 3% improvement over WebRTC and a 0.3% improvement against R3Net v1.4 in terms of video MOS. The movement in video MOS is statistically significant. As for audio MOS, *Merlin* beats WebRTC and R3Net v1.4 by 0.4% and 1.7% respectively. While *Merlin* attains a modest improvement over state-of-the-art methods, we emphasize that *Merlin* is trained completely from offline experience while R3Net v1.4 required millions of online network interactions to converge and WebRTC involved extensive domain knowledge and hand-engineered rules to attain comparable performance. It is important to note that WebRTC, while the standard for RTC, is designed to be a general purpose RTC stack as opposed to specializing in videoconferencing. Due to its general purpose nature, UKF’s specialized estimates outperform WebRTC; hence, as the imitator, *Merlin* in turn outperforms WebRTC. In contrast, the performance gap between *Merlin* and R3Net v1.4 is likely due to limitations in generalizability. For example, while heuristic-based models like UKF were designed with domain expertise to ensure domain adaption, R3Net v1.4 was trained stochastically to maximize its reward, which may not fully map to user subjective experience across network settings.

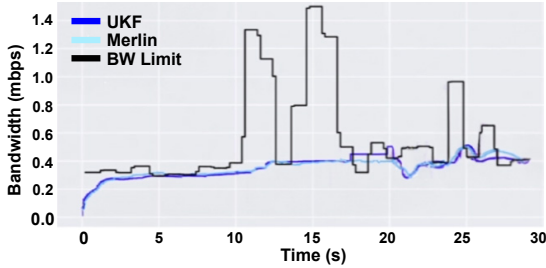
The evaluations further indicate that *Merlin* regresses in terms of the packet loss rate and delay mean against R3Net v1.4 and WebRTC respectively; however, *Merlin* attains a higher receiving rate which translates to more packets flowing across the network, triggering an increase in both the loss rate and delay mean. First, when the estimator produces higher estimates, a greater receiving rate can be attained. These esti-

mates are fed to the codec and the codec itself makes executive decisions such as assigning more parity packets to the link to mitigate packet loss through forward error correction (FEC). Thus, with a higher receiving rate, we can expect the loss rate and congestion to increase which degrades the delay metric. However, we emphasize that the 3 ms delay regression against WebRTC is negligible as it translates to a delay MOS increase of ≈ 0.001 . The movement in receiving rate and delay are statistically significant. Despite these regressions, *Merlin* enhances both video MOS and audio MOS, which are two established objective QoE metrics, when compared with WebRTC and R3Net v1.4.

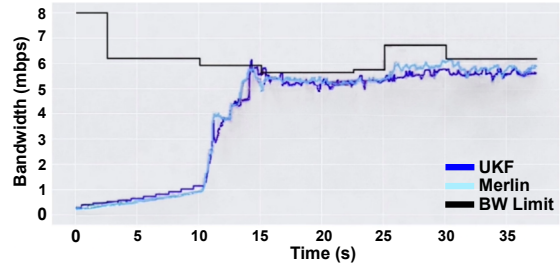
Lastly, we compare against UKF on our testbed environment to study how well *Merlin* imitates our expert. Quantitatively, in terms of video MOS, audio MOS, and the receiving rate, we observe no statistically significant movement across our production traces (see Table 1), which indicates that these metrics are statistically drawn from the same distribution. However, *Merlin* does incur a degradation in terms of both the loss rate and delay in comparison to UKF. While close, the small deviation in loss rate and delay may indicate that *Merlin* fails to entirely mimic our expert. One possible explanation for this regression is the domain shift between our simulated environment and the testbed environment. Since *Merlin* is trained entirely from offline simulated data, the delay metrics observed at train time may not fully match our target environment. This is because networks fall under the umbrella of partially observable environments as links outside the subnet cannot be probed directly. As a result, many of these factors cannot be accurately simulated within our simulated environment, leading to a divergence in delay metrics. One possible resolution would be to incorporate real-world data into our offline dataset, enabling *Merlin* to observe the shift in delay computation. Despite this regression, in terms of our gold standard MOS metrics, *Merlin* outperforms the state-of-the-art and demonstrates no statistical movement in comparison to the expert, demonstrating that *Merlin* is capable of generalizing to new environments from simulated, offline expert observations. Qualitative results are presented in Appendix C.

5.4 Videoconferencing in the Wild

We compare *Merlin* against WebRTC and UKF over real network links. We deploy and evaluate each estimator over real networks with links spanning multiple continents. We aggregate statistics from ≈ 2100 calls. Our results are summarized in Table 2 and Figure 9. The results demonstrate that *Merlin* is capable of generalizing from simulated to real-world environments, performing competitively with our expert UKF and WebRTC. We observe competitive audio MOS performance against both UKF and WebRTC, differing by 0.2% and 0.1% respectively. In terms of video MOS scores, *Merlin* regresses by 2.9% against UKF; however *Merlin* outperforms WebRTC by 3.75%. Similarly, *Merlin* leads to a



(a) Fluctuating Bandwidth.



(b) High Bandwidth.

Figure 7: Imitating UKF in Simulation.

0.4% boost against WebRTC and a 13% reduction in comparison to UKF in terms of the observed receiving rate. We note that `Merlin` achieves a higher median video MOS and receiving rate than UKF; however, UKF’s video MOS and receiving rate metrics exhibit higher variance compared to `Merlin` (see Appendix D). Although `Merlin` regresses, we emphasize the two following aspects. One, `Merlin` was trained purely from offline, simulated experience with zero network interactions and is able to outperform WebRTC and compete with UKF. Two, while we have not solved the problem of domain shift completely, `Merlin`’s data-driven design enables the potential to reduce the performance gap by incorporating more data and finetuning our objective function.

In contrast, the evaluations further indicate that `Merlin` improves in terms of the packet loss rate and delay against both UKF and WebRTC. The difference in observed metrics translates to a 19% and 42.85% loss rate improvement against UKF and WebRTC respectively. In terms of observed delay, `Merlin` achieves a 4.9% and 12.8% gain over UKF and WebRTC respectively. Similar to the previous evaluation, we emphasize that UKF achieves a higher receiving rate, leading to more packets entering the network and potentially increasing the packet loss and delay; however, in comparison to WebRTC, `Merlin` achieves a higher receiving rate while reducing both packet loss and delay which translates to improved QoE. We hypothesize that this performance regression is a direct result of WebRTC’s general purpose nature, resulting in regressions against more specialized methods (e.g., `Merlin`) for RTC applications such as videoconferencing.

Lastly, we show how well `Merlin`’s extracted policy generalizes to a real-world environment. Specifically, we observe no statistically significant movement of `Merlin` against UKF within a real environment, indicating that `Merlin` is retaining the expert policy obtained from simulated experience even within environments that differ significantly from our simulation. Overall, `Merlin` produces competitive bandwidth estimates with our expert UKF model, while outperforming WebRTC across various settings. Our evaluations demonstrate that `Merlin` is capable of generalizing to new environments from simulated, offline expert observations.

5.5 Guidance for Bandwidth Estimation

Impact of Features. We seek to study the impact of different features on learned BWE; specifically, handcrafted features with domain knowledge may impede our learned estimators.

We group features into five categories and ablate on these groups: receiving rate, loss ratio, average number of lost packets, queuing delay, and media type features. The media type features report the probability mass of video packets, audio packets, and screen sharing packets over the last three time steps. We then exhaustively retrain `Merlin` on each feature subset and report the performance on generated production traces within our simulated environment. We report our findings in Figure 10a. Our experiments indicate that the two most impactful features are the receiving rate and the media type features. Surprisingly, we find that the receiving rate feature alone is sufficient to mimic UKF with an action space MSE of ≈ 0.0028 . The impact of the receiving rate is expected, but the magnitude is unexpected. The receiving rate corresponds to the rate of information that the receiving endpoint is capable of receiving; hence, we would expect the receiving rate to correlate heavily with the throughput achieved at the bottleneck link.

Similarly, the media type feature alone enables `Merlin` to achieve approximate action space errors of 0.0037 in relation to UKF; in contrast, while the queuing delay feature bolsters our learned estimator, the queuing delay, loss ratio, and average loss features individually are insufficient to mimic our expert (see Appendix B). The ablation results further indicate that without either the receiving rate or media type features, `Merlin` is unable to learn a competitive BWE policy. One explanation is that both receive rate and media type features encode the observed audio and video receive rates. The receive rate feature reflects the combination of both audio and video receive rates, while the media type features provide estimates of the relative proportion of audio and video packets received over a given window. Depending on the workload, the proportion skew heavily influences bandwidth estimates. Since audio requires only 10 Kbps of resources, the flow of audio packets remains relatively constant; hence, when the video packet to audio packet proportion is high, link resources correspondingly are abundant to support the flow of high-quality video which is further corroborated by the impact of the video start times detailed in section 5.2. In combination, both the audio receive rate and video receive rate can be derived from these two features, which together help improve the quality of bandwidth estimates.

While loss metrics provide the agent with auxiliary information, by themselves they are noisy. We hypothesize that this discrepancy in performance stems directly from partial observability. For example, while packet loss may result from

Model	Video MOS	Audio MOS	Receiving Rate	Loss Rate	Delay Mean
Merlin	2.9150 ± 0.1538**	2.8598 ± 0.0821	849.9764 ± 104.4793**	0.0353 ± 0.0144	30.8500 ± 4.3147
UKF	2.9068 ± 0.2004	2.8401 ± 0.0795	829.7375 ± 127.6	0.0328 ± 0.0105	28.0160 ± 3.5423
WebRTC	2.8519 ± 0.1217	2.8452 ± 0.0667	775.3979 ± 60.2634	0.0375 ± 0.0053	26.1996 ± 2.5462**
R3Net v1.4	2.9050 ± 0.2438	2.8094 ± 0.0897	847.9143 ± 148.3244	0.0328 ± 0.0163	42.2350 ± 7.4667

Table 1: Benchmarking on Emulated Links. **Statistical significance with $p < 0.05$ between Merlin, WebRTC, and R3Net v1.4.

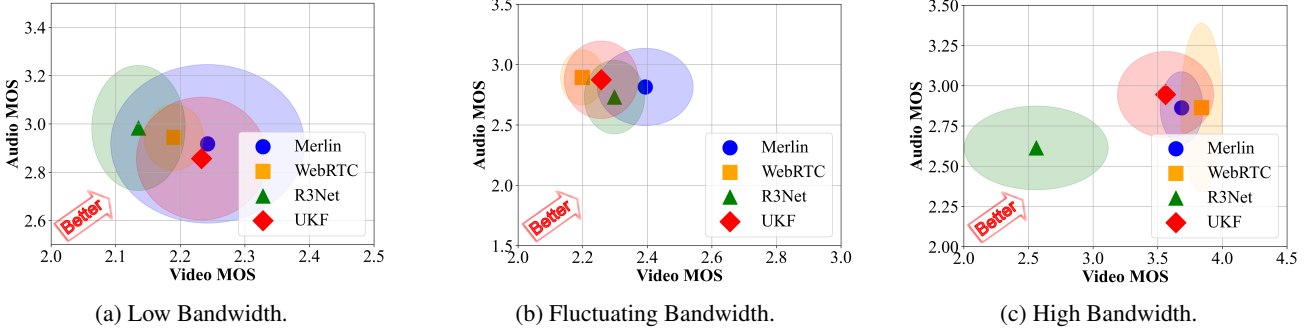


Figure 8: Video MOS vs. Audio MOS performance across emulated network environments.

Model	Video MOS	Audio MOS	Receiving Rate	Loss Rate	Delay Mean
Merlin	4.069 ± 0.6204	4.811 ± 0.1344	1910.521 ± 705.7378	0.0021 ± 0.0136	6.856 ± 26.7283
UKF	4.190 ± 0.3236	4.824 ± 0.1218	2159.809 ± 311.1544	0.0025 ± 0.0177	7.191 ± 15.5186
WebRTC	3.919 ± 0.4873	4.817 ± 0.1674	1901.152 ± 435.089	0.0030 ± 0.0183	7.730 ± 28.2775

Table 2: Benchmarking on Wild Networks.

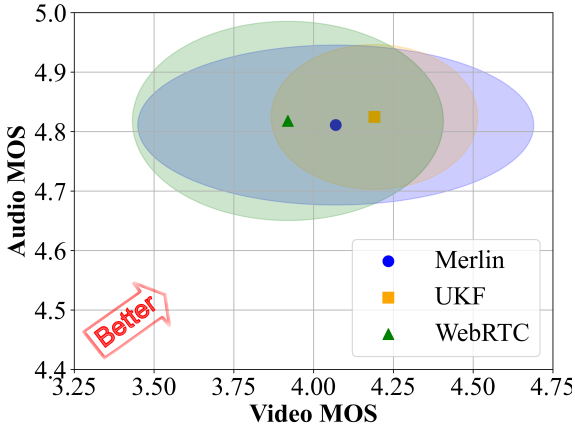
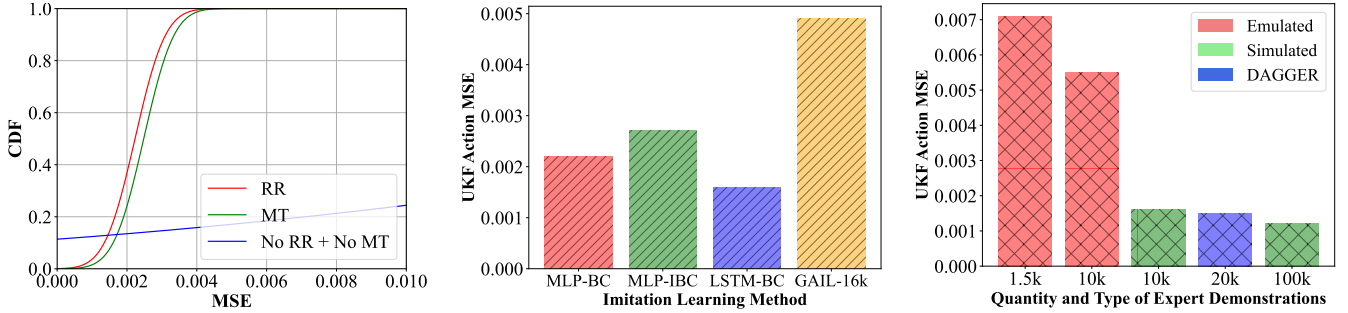


Figure 9: Video MOS vs. Audio MOS on Wild Networks.

network congestion and exhausted link resources, loss may additionally arise from physical factors, e.g., fading in wireless networks and link level disconnections— both of which are indistinguishable from the agent’s perspective and impact loss rates regardless of the bottleneck’s available resources. Lastly, we find that the best performing subset of features contains all five feature groups (see Appendix B for more details). It appears that the receiving rate, packet type, and delay-based features serve as core features and are crucial towards real-time BWE, while loss-based features appear to bolster performance but operate as auxiliary information.

Learning Methods and Architecture. We evaluate the performance of different IL methods and architectures for BWE

within our gym environment. We compare three different IL approaches: BC, Implicit Behavioral Cloning (IBC) [15], and Generative Adversarial Imitation Learning (GAIL) [20] and two policy architectures for BC: a multi-layer perceptron (MLP) and an LSTM. We report our findings in Figure 10b. We implement IBC and GAIL with MLP-based policy networks. We adopt similar hyperparameters for each model and maintain the same gym validation parameters across trials. We train GAIL with 16000 expert state-action samples per training epoch. Our evaluations indicate that BC with an LSTM policy network outperforms all other benchmarked methods, achieving an action MSE error of 0.0016 (see Figure 10b). The next best performing approach is BC with an MLP-based policy network, followed by IBC and then GAIL. We hypothesize that IBC and GAIL are more effective than BC in environments with limited expert demonstrations due to their joint representation of states and actions; however, in our case, we have an abundance of rich expert demonstrations and are effectively able to better cover our state space, mitigating the likelihood our imitator arrives at a previously unseen state which in turn reduces the effect of compounding error. Lastly, we ablate on the size of Merlin’s LSTM; however, we observe little performance difference between model sizes (see Appendix B). Given that Merlin produces a single output from 64 inputs, the problem is relatively small; hence, we would not expect model size to severely influence performance. In essence, when expert demonstrations are



(a) Imitation Performance with Different Feature Sets: Receive Rate subsets (RR); Media Type subsets (MT); No Receive Rate or Media Type features (No RR + No MT).

(b) Performance of various Imitation Learning methods for bandwidth estimation.

(c) Quantity and quality of demonstrations vs. imitation performance.

Figure 10: Ablation Study Results.

readily available, BC provides favorable results. Furthermore, exploiting temporal correlations present in network control tasks with recurrent networks appears to enhance policy performance.

Quantity and Quality of Demonstrations. We explore the impact of the quantity and quality of demonstrations on our learned estimator. Specifically, we compare with expert demonstrations drawn from two environments: our simulation and our testbed environment. We retrain `Merlin` on four different datasets: 1.5k emulated trajectories, 10k emulated trajectories, 10k simulated trajectories, and 100k simulated trajectories. The emulated trajectories are intentionally limited; that is, we do not randomize call parameters and leverage parameters drawn directly from production traces. By limiting the breadth of demonstrations from the target distribution, the relation between demonstration diversity and data quality can be explored. Emulated data is of higher quality as it reduces the domain shift between offline and online samples.

Furthermore, we evaluate the implications of DAGGER [45] on our 10k gym dataset, doubling the dataset size to 20k demonstrations by the end of the training run. We report our findings in Figure 10c. First, comparing the performance of `Merlin` on 10k emulated trajectories and 10k simulated trajectories, we observe greater gym performance with our simulated trajectories rather than our emulated demonstrations. `Merlin` achieves an action MSE error of 0.0016 with the simulated dataset in comparison to 0.0055 action MSE error with the emulated demonstrations. Furthermore, qualitatively, we observe that utilizing 10k simulated demonstrations is superior to training on 10k emulated demonstrations even when evaluating on our emulated platform (see Appendix C). We hypothesize that this robustness to domain shift is due to the reduction of compounding error; specifically, since our simulated dataset contains a richer set of trajectories, i.e., trajectories unlikely to be encountered in real deployments, `Merlin` is able to observe our expert across a more diverse set of circumstances which bolsters performance. Second, comparing the performance of 10k gym samples, 20k gym samples collected with DAGGER, and 100k gym samples,

we observe little added benefit within our gym environment. Our results indicate a modest improvement of 0.0003 in terms of action MSE with 80k extra demonstrations compared to DAGGER-enhanced training; however, when benchmarking each method on our testbed, we observe that the model trained with 100k demonstrations performs the best overall. While we observe that 10k demonstrations are sufficient to learn a BWE policy, increasing the number of expert observations appears to improve generalization. Furthermore, data diversity appears to impact imitation performance more than demonstration quality. Thus, to learn network control policies via offline expert demonstrations, we find that providing the agent with a large number of diverse demonstrations is key to ensuring robustness against domain shift which is corroborated in [60].

6 Conclusion

In our work, we tackle key challenges in adopting AI-based system optimization and control such as domain shift. Through our evaluations, we demonstrate `Merlin` as a data-driven solution that builds upon prior network control heuristics. We provide preliminary results demonstrating the promise of offline learning for learning real-time network control policies. Although `Merlin` learns a robust BWE policy and outperforms state-of-the-art rule-based and learning-based methods, `Merlin` is not the end for data-driven BWE. For example, we evaluate only audio and video calls in peer-to-peer setups; however, many videoconferencing calls consist of multiple endpoints communicating over group video calls which involve a single centralized server. As flows are concentrated at a single node, the complexity of BWE increases as competing receiver flows may impede one another. Furthermore, warm-starting RL agents with policies extracted from BC have been shown to produce strong results [36] which may translate to improved network control policies. We hope that `Merlin`'s offline-oriented design fosters new strategies for real-time network control.

Acknowledgements

We would like to thank Lili Qiu for her highly valuable feedback. We thank Scott Inglis and Ezra Ameri for their help.

References

- [1] Soheil Abbasloo, Chen-Yu Yen, and H Jonathan Chao. Classic meets modern: A pragmatic learning-based congestion control for the internet. In *Proceedings of the Annual conference of the ACM Special Interest Group on Data Communication on the applications, technologies, architectures, and protocols for computer communication*, pages 632–647, 2020.
- [2] Pieter Abbeel and Andrew Y Ng. Apprenticeship learning via inverse reinforcement learning. In *Proceedings of the twenty-first international conference on Machine learning*, page 1, 2004.
- [3] Abdelhak Bentaleb, Mehmet N Akcay, May Lim, Ali C Begen, and Roger Zimmermann. Bob: Bandwidth prediction for real-time communications using heuristic and reinforcement learning. *IEEE Transactions on Multimedia*, 2022.
- [4] A Bergkvist, D Burnett, C Jennings, and A Narayanan. Webrtc 1.0: Real-time communication between browsers. w3c working draft. *World Wide Web Consortium*, 2012.
- [5] Rajarshi Bhattacharyya, Archana Bura, Desik Rengaranjan, Mason Rumuly, Bainan Xia, Srinivas Shakkottai, Dileep Kalathil, Ricky KP Mok, and Amogh Dhamdhere. Qflow: A learning approach to high qoe video streaming at the wireless edge. *IEEE/ACM Transactions on Networking*, 30(1):32–46, 2021.
- [6] Neal Cardwell, Yuchung Cheng, C. Stephen Gunn, Soheil Hassas Yeganeh, and Van Jacobson. Bbr: Congestion-based congestion control: Measuring bottleneck bandwidth and round-trip propagation time. *Queue*, 14(5):20–53, oct 2016.
- [7] Gaetano Carlucci, Luca De Cicco, Stefan Holmer, and Saverio Mascolo. Analysis and design of the google congestion control for web real-time communication (WebRTC). In *Proceedings of the 7th International Conference on Multimedia Systems - MMSys '16*, pages 1–12, Klagenfurt, Austria, 2016. ACM Press.
- [8] Ke Chen, Han Wang, Shuwen Fang, Xiaotian Li, Minghao Ye, and H Jonathan Chao. RI-afec: adaptive forward error correction for real-time video communication based on reinforcement learning. In *Proceedings of the 13th ACM Multimedia Systems Conference*, pages 96–108, 2022.
- [9] R. Droms. Automated configuration of tcp/ip with dhcp. *IEEE Internet Computing*, 3(4):45–53, 1999.
- [10] Zhuoxuan Du, Jiaqi Zheng, Hebin Yu, Lingtao Kong, and Guihai Chen. A unified congestion control framework for diverse application preferences and network conditions. In *Proceedings of the 17th International Conference on emerging Networking EXperiments and Technologies*, pages 282–296, 2021.
- [11] Salma Emara, Baochun Li, and Yanjiao Chen. Eagle: Refining congestion control by learning from the experts. In *IEEE INFOCOM 2020-IEEE Conference on Computer Communications*, pages 676–685. IEEE, 2020.
- [12] Jeongyoon Eo, Zhixiong Niu, Wenxue Cheng, Francis Y Yan, Rui Gao, Jorina Kardhashi, Scott Inglis, Michael Revow, Byung-Gon Chun, Peng Cheng, et al. Opennetlab: Open platform for rl-based congestion control for real-time communications. *Proc. of APNet*, 2022.
- [13] Joyce Fang, Martin Ellis, Bin Li, Siyao Liu, Yasaman Hosseinkashi, Michael Revow, Albert Sadovnikov, Ziyuan Liu, Peng Cheng, Sachin Ashok, David Zhao, Ross Cutler, Yan Lu, and Johannes Gehrke. Reinforcement learning for bandwidth estimation and congestion control in real-time communications. 2019. arXiv:1912.02222 [cs].
- [14] Chelsea Finn, Sergey Levine, and Pieter Abbeel. Guided cost learning: Deep inverse optimal control via policy optimization. In *International conference on machine learning*, pages 49–58. PMLR, 2016.
- [15] Pete Florence, Corey Lynch, Andy Zeng, Oscar A Ramirez, Ayzaan Wahid, Laura Downs, Adrian Wong, Johnny Lee, Igor Mordatch, and Jonathan Tompson. Implicit behavioral cloning. In *Conference on Robot Learning*, pages 158–168. PMLR, 2022.
- [16] Sadjad Fouladi, John Emmons, Emre Orbay, Catherine Wu, Riad S Wahby, and Keith Winstein. Salsify: {Low-Latency} network video through tighter integration between a video codec and a transport protocol. In *15th USENIX Symposium on Networked Systems Design and Implementation (NSDI 18)*, pages 267–282, 2018.
- [17] Justin Fu, Katie Luo, and Sergey Levine. Learning robust rewards with adversarial inverse reinforcement learning. *arXiv preprint arXiv:1710.11248*, 2017.
- [18] Benjamin Fuhrer, Yuval Shpigelman, Chen Tessler, Shie Mannor, Gal Chechik, Eitan Zahavi, and Gal Dalal. Implementing reinforcement learning datacenter congestion control in nvidia nics. In *2023 IEEE/ACM 23rd International Symposium on Cluster, Cloud and Internet Computing (CCGrid)*, pages 331–343, 2023.

- [19] Dylan Hadfield-Menell, Smitha Milli, Pieter Abbeel, Stuart J Russell, and Anca Dragan. Inverse reward design. *Advances in neural information processing systems*, 30, 2017.
- [20] Jonathan Ho and Stefano Ermon. Generative adversarial imitation learning. *Advances in neural information processing systems*, 29, 2016.
- [21] Ningning Hu and Peter Steenkiste. Estimating available bandwidth using packet pair probing. Technical report, CARNEGIE-MELLON UNIV PITTSBURGH PA SCHOOL OF COMPUTER SCIENCE, 2002.
- [22] Tianchi Huang, Rui-Xiao Zhang, Chao Zhou, and Lifeng Sun. Qarc: Video quality aware rate control for real-time video streaming based on deep reinforcement learning. In *Proceedings of the 26th ACM international conference on Multimedia*, pages 1208–1216, 2018.
- [23] Tianchi Huang, Chao Zhou, Lianchen Jia, Rui-Xiao Zhang, and Lifeng Sun. Learned internet congestion control for short video uploading. In *Proceedings of the 30th ACM International Conference on Multimedia*, pages 3064–3075, 2022.
- [24] Nathan Jay, Noga Rotman, Brighten Godfrey, Michael Schapira, and Aviv Tamar. A deep reinforcement learning perspective on internet congestion control. In Kamalika Chaudhuri and Ruslan Salakhutdinov, editors, *Proceedings of the 36th International Conference on Machine Learning*, volume 97 of *Proceedings of Machine Learning Research*, pages 3050–3059. PMLR, 09–15 Jun 2019.
- [25] Nathan Jay, Noga Rotman, Brighten Godfrey, Michael Schapira, and Aviv Tamar. A deep reinforcement learning perspective on internet congestion control. In *International Conference on Machine Learning*, pages 3050–3059. PMLR, 2019.
- [26] Wonseok Jeon, Seokin Seo, and Kee-Eung Kim. A bayesian approach to generative adversarial imitation learning. *Advances in neural information processing systems*, 31, 2018.
- [27] Ingemar Johansson. Self-clocked rate adaptation for conversational video in lte. In *Proceedings of the 2014 ACM SIGCOMM workshop on Capacity sharing workshop*, pages 51–56, 2014.
- [28] Sukhpreet Kaur Khangura and Sami Akin. Online available bandwidth estimation using multiclass supervised learning techniques. *Computer Communications*, 170:177–189, 2021.
- [29] Akira Kinose and Tadahiro Taniguchi. Integration of imitation learning using gail and reinforcement learning using task-achievement rewards via probabilistic graphical model. *Advanced Robotics*, 34(16):1055–1067, 2020.
- [30] Insoo Lee, Seyeon Kim, Sandesh Sathyanarayana, Kyungmin Bin, Song Chong, Kyunghan Lee, Dirk Grunwald, and Sangtae Ha. R-fec: RI-based fec adjustment for better qoe in webrtc. In *Proceedings of the 30th ACM International Conference on Multimedia*, pages 2948–2956, 2022.
- [31] Sergey Levine and Vladlen Koltun. Continuous inverse optimal control with locally optimal examples. *arXiv preprint arXiv:1206.4617*, 2012.
- [32] Sergey Levine, Zoran Popovic, and Vladlen Koltun. Nonlinear inverse reinforcement learning with gaussian processes. *Advances in neural information processing systems*, 24, 2011.
- [33] Haoyong Li, Bingcong Lu, Jun Xu, Li Song, Wenjun Zhang, Lin Li, and Yaoyao Yin. Reinforcement learning based cross-layer congestion control for real-time communication. In *2022 IEEE International Symposium on Broadband Multimedia Systems and Broadcasting (BMSB)*, pages 01–06, 2022.
- [34] Haoyong Li, Bingcong Lu, Jun Xu, Li Song, Wenjun Zhang, Lin Li, and Yaoyao Yin. Reinforcement learning based cross-layer congestion control for real-time communication. In *2022 IEEE International Symposium on Broadband Multimedia Systems and Broadcasting (BMSB)*, pages 01–06. IEEE, 2022.
- [35] Haoyong Li, Bingcong Lu, Jun Xu, Li Song, Wenjun Zhang, Lin Li, and Yaoyao Yin. Reinforcement learning based cross-layer congestion control for real-time communication. In *2022 IEEE International Symposium on Broadband Multimedia Systems and Broadcasting (BMSB)*, pages 01–06. IEEE, 2022.
- [36] Jianxiong Li, Xiao Hu, Haoran Xu, Jingjing Liu, Xianyuan Zhan, and Ya-Qin Zhang. Proto: Iterative policy regularized offline-to-online reinforcement learning. *arXiv preprint arXiv:2305.15669*, 2023.
- [37] Qiong Liu, Peng Yang, Feng Lyu, Ning Zhang, and Li Yu. Multi-objective network congestion control via constrained reinforcement learning. In *2021 IEEE Global Communications Conference (GLOBECOM)*, pages 1–6. IEEE, 2021.
- [38] Hongzi Mao, Shannon Chen, Drew Dimmery, Shaun Singh, Drew Blaisdell, Yuandong Tian, Mohammad Alizadeh, and Eytan Bakshy. Real-world video adaptation with reinforcement learning. *arXiv preprint arXiv:2008.12858*, 2020.

- [39] Hongzi Mao, Ravi Netravali, and Mohammad Alizadeh. Neural Adaptive Video Streaming with Pensieve. In *Proceedings of the Conference of the ACM Special Interest Group on Data Communication - SIGCOMM '17*, pages 197–210, Los Angeles, CA, USA, 2017. ACM Press.
- [40] Hongzi Mao, Ravi Netravali, and Mohammad Alizadeh. Neural adaptive video streaming with pensieve. In *Proceedings of the conference of the ACM special interest group on data communication*, pages 197–210, 2017.
- [41] Gabriel Mittag, Babak Naderi, Vishak Gopal, and Ross Cutler. Lstm-based video quality prediction accounting for temporal distortions in videoconferencing calls. In *ICASSP 2023-2023 IEEE International Conference on Acoustics, Speech and Signal Processing (ICASSP)*, pages 1–5. IEEE, 2023.
- [42] Andrew Y Ng, Stuart Russell, et al. Algorithms for inverse reinforcement learning. In *Icml*, volume 1, page 2, 2000.
- [43] Ali Rezagholizadeh. *Source rate control in videoconferencing application using state-action-reward-state-action temporal difference reinforcement learning*. PhD thesis, École de technologie supérieure, 2022.
- [44] George F Riley and Thomas R Henderson. The ns-3 network simulator. In *Modeling and tools for network simulation*, pages 15–34. Springer, 2010.
- [45] Stephane Ross, Geoffrey Gordon, and Drew Bagnell. A reduction of imitation learning and structured prediction to no-regret online learning. In Geoffrey Gordon, David Dunson, and Miroslav Dudík, editors, *Proceedings of the Fourteenth International Conference on Artificial Intelligence and Statistics*, volume 15 of *Proceedings of Machine Learning Research*, pages 627–635, Fort Lauderdale, FL, USA, 11–13 Apr 2011. PMLR.
- [46] Henning Schulzrinne, Stephen Casner, Ron Frederick, and Van Jacobson. Rtp: A transport protocol for real-time applications. Technical report, 2003.
- [47] Sadia J Siddiqi, Faisal Naeem, Saud Khan, Komal S Khan, and Muhammad Tariq. Towards ai-enabled traffic management in multipath tcp: A survey. *Computer Communications*, 181:412–427, 2022.
- [48] Viswanath Sivakumar, Olivier Delalleau, Tim Rocktäschel, Alexander H Miller, Heinrich Küttler, Nantas Nardelli, Mike Rabbat, Joelle Pineau, and Sebastian Riedel. Mvfst-rl: An asynchronous rl framework for congestion control with delayed actions. *arXiv preprint arXiv:1910.04054*, 2019.
- [49] Mingfei Sun and Xiaojuan Ma. Adversarial imitation learning from incomplete demonstrations. *arXiv preprint arXiv:1905.12310*, 2019.
- [50] Umar Syed, Michael Bowling, and Robert E Schapire. Apprenticeship learning using linear programming. In *Proceedings of the 25th international conference on Machine learning*, pages 1032–1039, 2008.
- [51] Umar Syed and Robert E Schapire. A game-theoretic approach to apprenticeship learning. *Advances in neural information processing systems*, 20, 2007.
- [52] Chen Tessler, Yuval Shpigelman, Gal Dalal, Amit Mandelbaum, Doron Haritan Kazakov, Benjamin Fuhrer, Gal Chechik, and Shie Mannor. Reinforcement learning for datacenter congestion control. *SIGMETRICS Perform. Eval. Rev.*, 49(2):43–46, jan 2022.
- [53] Faraz Torabi, Garrett Warnell, and Peter Stone. Behavioral cloning from observation. *arXiv preprint arXiv:1805.01954*, 2018.
- [54] Bo Wang, Yuan Zhang, Size Qian, Zipeng Pan, and Yuhong Xie. A hybrid receiver-side congestion control scheme for web real-time communication. In *Proceedings of the 12th ACM Multimedia Systems Conference*, pages 332–338, 2021.
- [55] Wenting Wei, Huaxi Gu, and Baochun Li. Congestion control: A renaissance with machine learning. *IEEE Network*, 35(4):262–269, 2021.
- [56] Keith Winstein, Anirudh Sivaraman, and Hari Balakrishnan. Stochastic forecasts achieve high throughput and low delay over cellular networks. In *10th USENIX Symposium on Networked Systems Design and Implementation (NSDI 13)*, pages 459–471, 2013.
- [57] Zhenchang Xia, Libing Wu, Fei Wang, Xudong Liao, Haiyan Hu, Jia Wu, and Dan Wu. Glider: rethinking congestion control with deep reinforcement learning. *World Wide Web*, 26(1):115–137, 2023.
- [58] Xuedou Xiao, Mingxuan Yan, Yingying Zuo, Boxi Liu, Paul Ruan, Yang Cao, and Wei Wang. From ember to blaze: Swift interactive video adaptation via meta-reinforcement learning. *arXiv preprint arXiv:2301.05541*, 2023.
- [59] Francis Y Yan, Hudson Ayers, Chenzhi Zhu, Sadjad Fouladi, James Hong, Keyi Zhang, Philip Levis, and Keith Winstein. Continual learning improves internet video streaming. *arXiv preprint arXiv:1906.01113*, 2019.

- [60] Chen-Yu Yen, Soheil Abbasloo, and H. Jonathan Chao. Computers can learn from the heuristic designs and master internet congestion control. In *Proceedings of the ACM SIGCOMM 2023 Conference*, ACM SIGCOMM '23, page 255–274, New York, NY, USA, 2023. Association for Computing Machinery.
- [61] Tianrun Yin, Hongyu Wu, Runyu He, Shushu Yi, and Dingwei Li. Gemini: An ensemble framework for bandwidth estimation in web real-time communications.
- [62] Wenpei Yin, Bingcong Lu, Yan Zhao, Jun Xu, Li Song, and Wenjun Zhang. Safr: A real-time communication system with adaptive frame rate. In *Proceedings of the 1st International Workshop on Networked AI Systems*, pages 1–6, 2023.
- [63] Huanhuan Zhang, Anfu Zhou, Yuhan Hu, Chaoyue Li, Guangping Wang, Xinyu Zhang, Huadong Ma, Leilei Wu, Aiyun Chen, and Changhui Wu. Loki: improving long tail performance of learning-based real-time video adaptation by fusing rule-based models. In *Proceedings of the 27th Annual International Conference on Mobile Computing and Networking*, pages 775–788, 2021.
- [64] Huanhuan Zhang, Anfu Zhou, Jiamin Lu, Ruoxuan Ma, Yuhan Hu, Cong Li, Xinyu Zhang, Huadong Ma, and Xiaojiang Chen. Onrl: improving mobile video telephony via online reinforcement learning. In *Proceedings of the 26th Annual International Conference on Mobile Computing and Networking*, pages 1–14, 2020.
- [65] Kaizhe Zhang, Zhiwen Wang, Hansen Ma, Haipeng Du, and Weizhan Zhang. Hybridrts: A hybrid congestion control framework with rule and reinforcement learning for low-latency webRTC live video streaming. In *2022 IEEE 24th Int Conf on High Performance Computing & Communications; 8th Int Conf on Data Science & Systems; 20th Int Conf on Smart City; 8th Int Conf on Dependability in Sensor, Cloud & Big Data Systems & Application (HPCC/DSS/SmartCity/DependSys)*, pages 1757–1764. IEEE, 2022.
- [66] Lei Zhang, Yong Cui, Mowei Wang, Kewei Zhu, Yibo Zhu, and Yong Jiang. Deepcc: Bridging the gap between congestion control and applications via multiobjective optimization. *IEEE/ACM Transactions on Networking*, 2022.
- [67] Lei Zhang, Kewei Zhu, Junchen Pan, Hang Shi, Yong Jiang, and Yong Cui. Reinforcement learning based congestion control in a real environment. In *2020 29th International Conference on Computer Communications and Networks (ICCCN)*, pages 1–9. IEEE, 2020.
- [68] Anfu Zhou, Huanhuan Zhang, Guangyuan Su, Leilei Wu, Ruoxuan Ma, Zhen Meng, Xinyu Zhang, Xiufeng Xie, Huadong Ma, and Xiaojiang Chen. Learning to coordinate video codec with transport protocol for mobile video telephony. In *The 25th Annual International Conference on Mobile Computing and Networking*, pages 1–16, 2019.
- [69] Xiaoqing Zhu and Rong Pan. Nada: A unified congestion control scheme for low-latency interactive video. In *2013 20th International Packet Video Workshop*, pages 1–8. IEEE, 2013.
- [70] Brian D Ziebart, J Andrew Bagnell, and Anind K Dey. Modeling interaction via the principle of maximum causal entropy. 2010.
- [71] Brian D Ziebart, Andrew L Maas, J Andrew Bagnell, Anind K Dey, et al. Maximum entropy inverse reinforcement learning. In *Aaai*, volume 8, pages 1433–1438. Chicago, IL, USA, 2008.

A State Construction

See Table 3 for feature state construction.

Metric	Window Size
Receiving Rate	5
Long Term Receiving Rate	
Average Queue Time	
Long Term Average Queue Time	
Loss Ratio	
Long Term Loss Ratio	
Average Loss Packet	
Long Term Average Loss Packet	
Ratio of Video Packets	3
Long Term Ratio of Video Packets	
Ratio of Audio Packets	
Long Term Ratio of Audio Packets	
Ratio of Screenshare Packets	
Long Term Ratio of Screenshare Packets	
Ratio of Probe Packets	
Long Term Ratio of Probe Packets	

Table 3: Merlin State Construction. Short term metrics are sampled every 60 ms, while longer-term metrics are sampled every 600 ms.

B Simulated Evaluation

LSTM ablation results presented in Table 4. Feature set ablations detailed in Figure 11.

LSTM Neurons	Action MSE
32	0.0016
64	0.0016
128	0.0014
256	0.0016
512	0.0016
1024	0.0016

Table 4: Impact of LSTM size on imitation performance.

C Emulated Evaluation

Qualitative imitation performance of Merlin on real networks with emulated links presented in Figure 12. Impact of quality of demonstrations for BWE illustrated in Figure 13.

D Live Evaluation

Distribution of objective QoE metrics during inter-continental videoconferencing calls presented in Figure 14.

E Reinforcement Learning and Learning from Demonstrations

Reinforcement Learning. RL seeks to learn a policy for acting in an environment where the environment is represented by a Markov decision process (MDP). Given a set of states S and actions A , an agent seeks to learn a mapping between states and actions $\pi : A \times S \rightarrow [0, 1]$. Furthermore, the transition model defines the probability of a taking an action given the current state: $\pi(a, s) = Pr(a_t = a | s_t = s)$. We call the combination of the mapping and the transition model the policy— a conditional distribution of actions and states. To learn the desired policy, the agent seeks to maximize a reward metric that encodes the task goal. Agents are trained online for episodes of length t , estimating the expected reward at each step. The expected return is represented as $V_\pi(s) = E[R|s_0 = s] = E[\sum_{t=0}^{\infty} \gamma^t r_t | s_0 = s]$ where γ is referred to as the discount rate, which prioritizes events in the immediate future. By maximizing the expected return, the agent prioritizes states with higher expected rewards, guiding the agent toward a policy that accomplishes the desired task. However, mapping objective metrics to subjective metrics is still an area of active research; hence, designing comprehensive reward functions is hard. Accordingly, these challenges have spurred research in IL where a policy is extracted purely from expert demonstration. IL can loosely be categorized into inverse reinforcement learning (IRL), apprenticeship learning, and BC.

Inverse Reinforcement Learning. Early motivations of IRL stemmed from tasks in which reward functions were ill-defined, e.g., teaching a robot to pick up a box. Rather than handcrafting a reward function, early works sought to leverage expert demonstrations to derive a reward function via linear programming [42]. However, in many cases, the set of functions that describe a task is infinite, which makes derivation difficult, e.g., the trivial solution of $f(x) = 0$ satisfies most tasks [71]. In response to these difficulties, researchers turned toward entropy-based methods [70, 71]. That is, rather than searching over an unrestricted set of reward functions, the search space is constrained to policies that are “close” to the expert. Early works sought to match feature expectations, i.e., the agent arrives at similar states as the expert [32]. To accomplish this, the authors maintain close proximity to the expert policy via KL divergence and maximize the entropy of the learned policy to combat noise and partial observability present in expert demonstrations. Thus, the goal is to learn the worst policy that remains close to the expert. It is important to note that many of these works rely on the presupposition that the observed expert is optimal in regard to the observed task. Multiple works build on this notion of maximum entropy to take into account contextual information, e.g., previously visited states and actions, improving the runtime complexity, and relaxing the constraint that demonstrations are optimal [31, 70]. More recently, researchers have turned

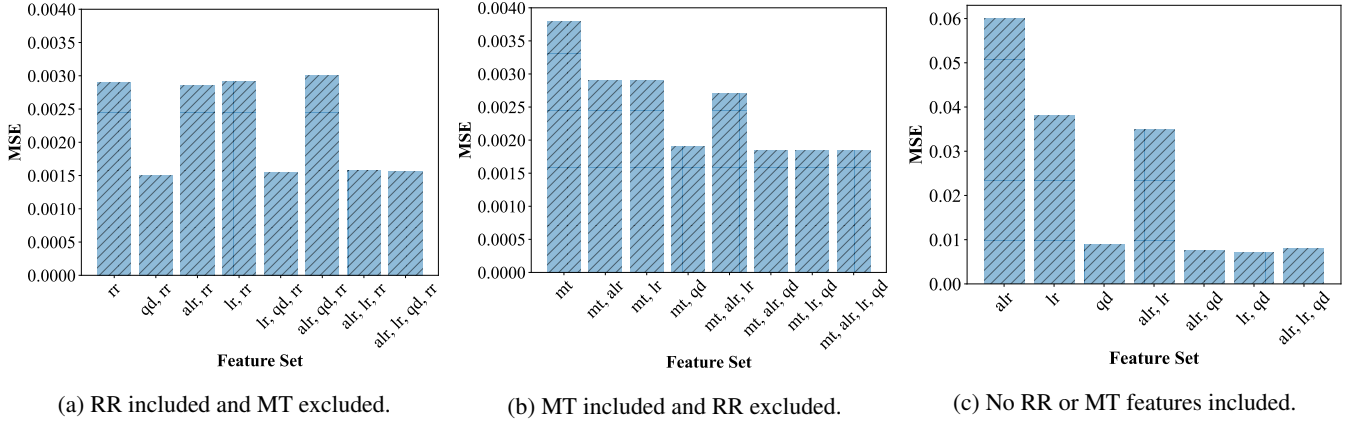


Figure 11: Imitation MSE per Feature Group: receive rate (rr), media type (mt), delay (qd), loss rate (lr), average loss rate (alr). Note the difference in axis scale.

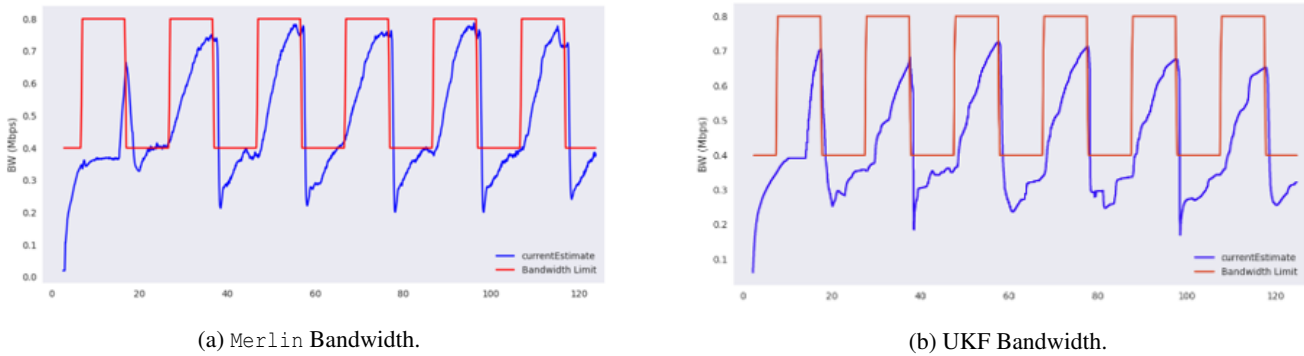


Figure 12: Imitating expert bandwidth predictions on emulated links with 100k training samples.

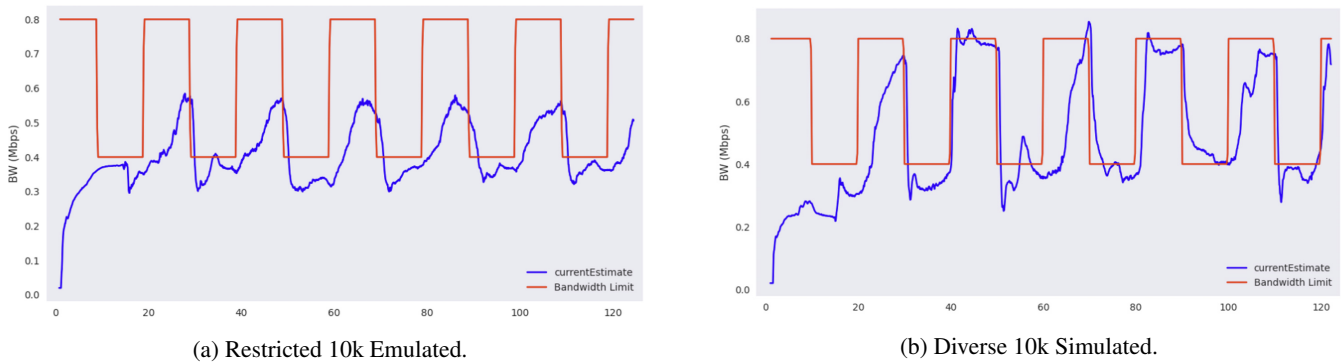


Figure 13: Quality of Demonstrations vs. Observed BWE Performance.

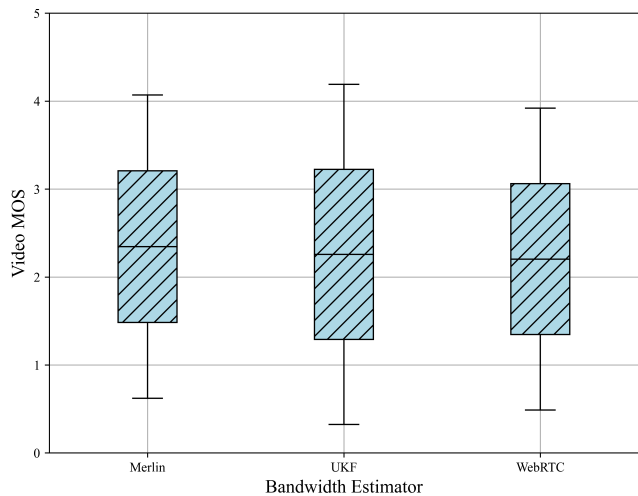
towards learned feature representations to enable rich reward extraction [14]. Adversarial Inverse Reinforcement Learning (AIRL) [17], the state-of-the-art IRL method, builds on many of the previously mentioned ideas but utilizes adversarial learning to derive and extract the expert reward. Although AIRL facilitates offline learning and robust reward extraction, IRL relies on executing RL within an "inner loop." That is,

each sample corresponds to an entire training episode which leads to extremely long runtimes and many environmental interactions.

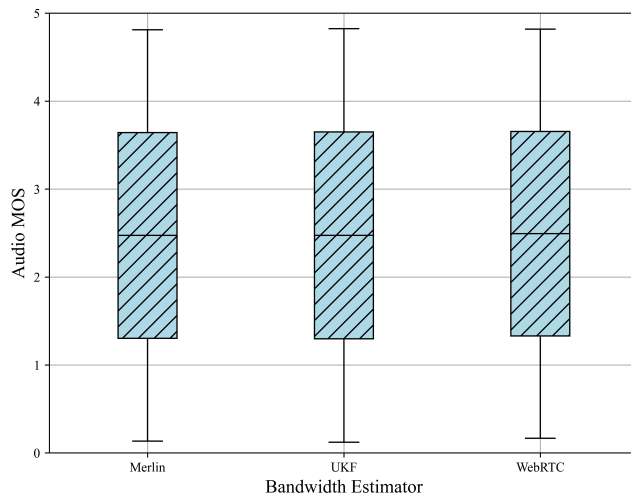
Apprenticeship Learning. In contrast to IRL, apprenticeship learning seeks to learn a policy directly by matching feature expectations [2]. Proponents of apprenticeship learning note the following insight: the reward function depends on

feature expectations; hence, the reward is encoded implicitly. Early works sought to leverage various optimization techniques to extract an expert policy [50, 51]. In contrast, similar to AIRL, the predominant apprenticeship learning method is Generative Adversarial Imitation Learning (GAIL) [20]. Unlike AIRL, GAIL is not an IRL technique, rather it learns a policy directly through distribution matching. GAIL leverages two neural networks in a GAN setup with the generator learning to produce a policy and the discriminator learning to discriminate between the imitator’s policy distribution and the expert’s. Many works have extended GAIL by handling incomplete demonstrations, altering the objective metric, and adding conditional goals [26, 29, 49]. GAIL remains a robust method in low data regimes; however, in settings where expert demonstrations are abundant, GAIL does not perform as well as competing methods such as BC [14].

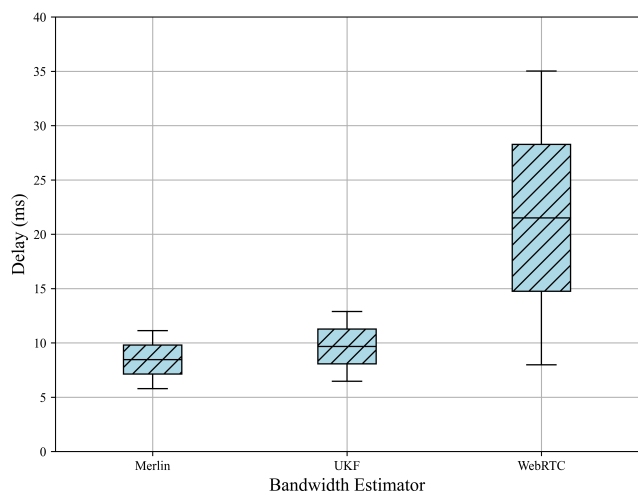
Behavioral Cloning. BC diverges from both apprenticeship learning and IRL in that it does not require iteratively running RL. BC runs purely from offline data, reframing the IL problem as supervised learning. That is, given an offline dataset of expert states and actions, BC learns an explicit mapping between expert state and action pairs. Given that traditional BC does not require querying an expert or interacting with an environment, training is often less expensive in comparison to its IL counterparts. Similarly, BC benefits from the well-studied discipline of supervised learning and inherits many of the convergence guarantees [53]. However, there is no free lunch. BC, although simple, suffers from the problem of compounding error [15]. That is, supervised learning tends to rely on the i.i.d assumption that each data observation is independent. However, when observing an expert complete a task, trajectory samples are not independent and often exhibit temporal dependence. As a result, when a BC model experiences an unfamiliar state, it produces an error. These errors compound over the task trajectory due to the temporal dependence between actions. To accommodate this, implicit methods have been proposed to alleviate compounding error by learning a joint distribution of states and actions [15]. Other methods such as DAGGER [45] have sought to expand the demonstration dataset and increase state space coverage. All in all, in low data regimes, BC tends to perform poorly due to compounding errors.



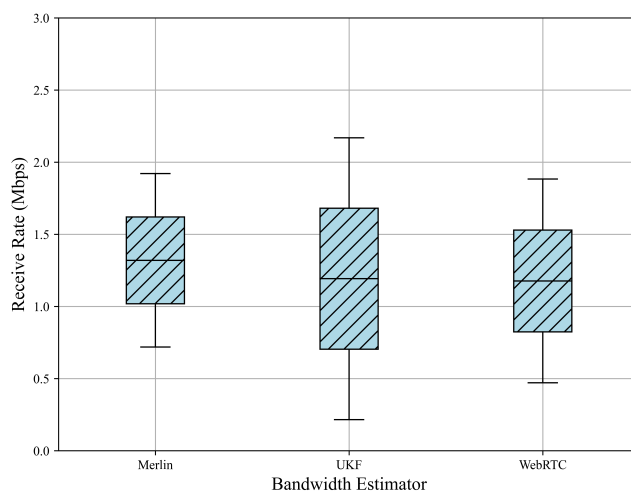
(a) Video MOS Distribution.



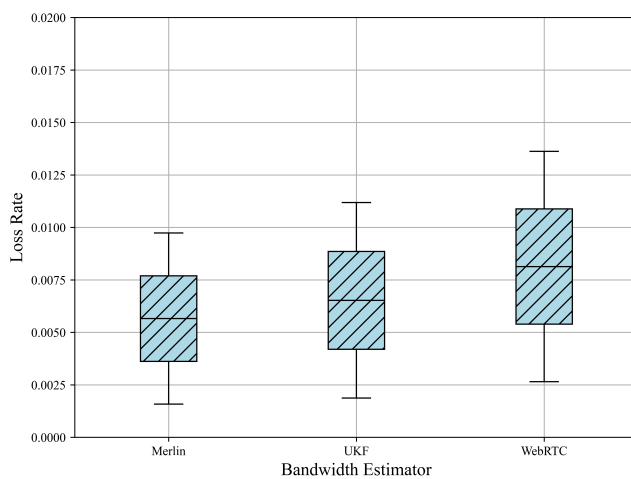
(b) Audio MOS Distribution.



(c) Delay Distribution.



(d) Receive Rate Distribution.



(e) Loss Rate Distribution.

Figure 14: Distribution of Objective Metrics over Inter-continental Links.